Queen's University
Belfast

A Statistical Characterization of Shadowed Fading in Indoor Off-Body Communications Channels At 5.8 GHz

Yoo, S. K., & Cotton, S. L. (2015). A Statistical Characterization of Shadowed Fading in Indoor Off-Body Communications Channels At 5.8 GHz. In Proceedings of 9th European Conference on Antennas and Propagation (EuCAP 2015). Institute of Electrical and Electronics Engineers (IEEE).

Published in:
Proceedings of 9th European Conference on Antennas and Propagation (EuCAP 2015)

Document Version:
Peer reviewed version

Queen's University Belfast - Research Portal:
Link to publication record in Queen's University Belfast Research Portal

A Statistical Characterization of Shadowed Fading in Indoor Off-Body Communications Channels at 5.8 GHz

Seong Ki Yoo and Simon L. Cotton

Institute of Electronics, Communication & Information Technology, Queen's University Belfast, BT3 9DT, UK

{syoo02, simon.cotton}@qub.ac.uk

Abstract—**This paper investigates the characteristics of the shadowed fading observed in off-body communications channels at 5.8 GHz using the *κ-µ* / gamma composite fading model. Realistic measurements have been conducted considering four individual scenarios namely line of sight (LOS) and non-LOS (NLOS) walking, rotation and random movements within an indoor laboratory environment. It is shown that the *κ-µ* / gamma composite fading model provides a better fit to the fading observed in off-body communications channels compared to the conventional Nakagami-*m* and Rician fading models.**

Index Terms— **body shadowing, *κ-µ* / gamma composite fading model, off-body communications channels, shadowed fading model.**

I. INTRODUCTION

The past few decades have witnessed significant research activity on the characterization and modeling of off-body communications channels [1-4]. However, none of these consider fading models which characterize the small-scale fading and shadowing (or random variation of the mean signal power) which exist concurrently. To this end, composite fading models, which are also called shadowed fading models, have been proposed [5-7].

Composite fading models can be broadly categorized into two groups according to the type of shadowing effect. The first group assumes that the line-of-sight (LOS) or dominant component is subject to random shadowing [5]. The other group assumes that the faded signal undergoes *multiplicative* shadowing. This occurs as a result of the random variation of the total power of the multipath components including both the LOS and scattered components [6, 7] because not only the LOS but also scatter components are randomly shadowed. Both composite fading models in [6, 7] are mixture of the Rayleigh and lognormal distributions. However, the former assumes that the mean-squared power of the fading amplitude follows a lognormal distribution [6] whereas the latter assumes that the root mean squared (*rms*) power of the fading amplitude varies according to a lognormal distribution [7]. Likewise, for *multiplicative* shadowing, either mean-squared power or *rms* power can

equivalently be assumed to follow an appropriate statistical distribution.

A new model for shadowed body centric communications channels was proposed in [8] under the assumption that the scattered components experience *κ-µ* fading [9] whereas shadowing of the resultant dominant component follows the lognormal distribution. For the validation of this new model, the measured and simulated shadowed body centric channels including on-, off- and body-to-body communications channels were used. As the Rice fading model appears as a special case of the *κ-µ* fading model, this new model contains Loo's shadowed fading model [5] as a special case. However, like Loo's model, the presence of the lognormal distribution in the model proposed in [8] often leads to mathematical expressions which are cumbersome to handle when additional operations are required.

As a result, another new shadowed fading model was proposed simultaneously in [10] and [11] which assumes that the shadowing of the resultant dominant component varies according to a Nakagami-*m* distribution. This approach has led to the derivation of closed-form expressions for the probability density function (PDF) of the model. It is also noted that these fading models [5, 8, 10, 11] were derived based on the assumption that the shadowing of dominant signal component, referred to as LOS shadowing, varies according to either a lognormal or Nakagami-*m* distribution. While this assumption may hold in some cases, it is not unreasonable to assume that both the dominant and scattered components may undergo shadowing together. To this effect, in this paper, for the first time, we perform a statistical characterization of shadowed fading for indoor off-body communications at 5.8 GHz using the *κ-µ* / gamma composite fading model [12].

II. EXPERIMENT SYSTEM AND MEASUREMENTS

A. Experiment System

The transmitter section of the channel measurement system consisted of an ML5805 transceiver, manufactured by RFMD, which was configured to transmit a +21 dBm continuous wave signal at 5.8 GHz. The transmit antenna

was mounted parallel to the body surface. The test subject was an adult male of height 1.83 m and mass of 73 kg. During the measurements, the transmitter was alternated between three different body locations on the test subject as shown in Fig. 1(a): the central chest region at a height of 1.42 m; the central waist region at a height of 1.15 m; the right wrist region at a height of 0.98 m. Please note that the transmit antenna was placed directly on the test subject without the use of a dielectric spacer.

The receiver section of the channel measurement system consisted of a sleeve dipole antenna which was connected to port 1 of a Rohde & Schwarz ZVB-8 Vector Network Analyzer (VNA) using a low-loss coaxial cable. A pre-measurement calibration was performed, using a Rohde & Schwarz ZV-Z51 calibration unit, to reduce the effects of known system based errors. This also enabled the elimination of the effects of the power amplifier and cable loss. The VNA was configured as a sampling receiver, recording the b_1 wave quantity incident on port 1 at sample rate of 56 Hz. The receiver was mounted vertically on a PVC stand at an elevation of 1.10 m above the floor level. The antennas used by both the transmitter and receiver were +2.3 dBi omnidirectional sleeve dipole antennas (Mobile Mark model PSKN3-24/55S) and were vertically polarized.

B. Measurements

All measurements in this study were conducted in the Wireless Communication Laboratory (WCL) situated on the second floor of the institute of Electronics, Communications and Information Technology (ECIT) building at Queen's University Belfast in the United Kingdom shown in Fig. 1(b). The building mainly consisted of metal studded dry wall with a metal tiled floor covered with polypropylene-fiber, rubber backed carpet tiles, and a metal ceiling with mineral fiber tiles and recessed louvered luminaries suspended 2.7 m above floor level. The lab contained a number of chairs, boxes, lab equipment, metal cabinets and also desks constructed from medium density fiberboard. The measurement environment was unoccupied for the duration of the experiments facilitating pedestrian free off-body channel measurements.

Four individual scenarios deemed likely to be encountered in everyday life were considered. These were: walking in (1) LOS and (2) NLOS where the test subject walked towards and then away from the receiver in a straight line, respectively; (3) rotational movements, where the test subject rotated 360° in a clockwise direction from LOS through to the maximum shadowing condition before returning to LOS at the separation distances of 1 m, 5 m and 9 m from the receiver; (4) random movement, where the test subject walked randomly within a circle area with a radius of 1 m. Due to the limitation of space, measurements were conducted at the separation distance of 1 m, 5 m and 8 m for random movement scenario. For all scenarios, the individual measurement trials were repeated three times.
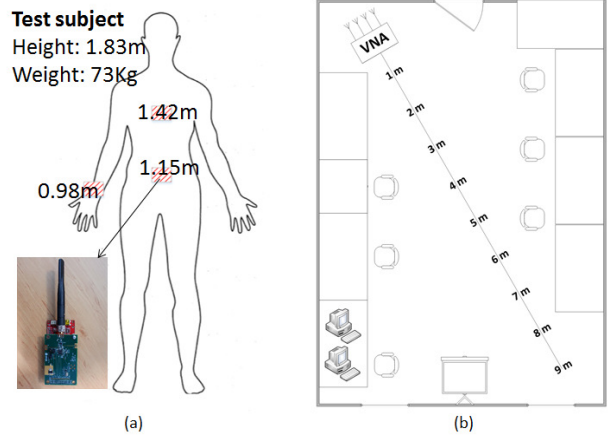

Fig. 1 (a) Measurement system showing three different transmitter locations and (b) indoor environment showing receiver location and measurement positions.

III. COMPOSITE FADING MODEL

The PDF of the κ-μ fading signal envelope R can be written as [9]

$$p_R(r) = \frac{1}{\hat{r}} \frac{2\mu(\kappa+1)^{\frac{\mu+1}{2}}}{\kappa^{\frac{\mu-1}{2}} e^{\mu\kappa} e^{\mu(\kappa+1)\left(\frac{r}{\hat{r}}\right)^2}} \left(\frac{r}{\hat{r}}\right)^\mu I_{\mu-1}\left(2\mu\sqrt{\kappa(\kappa+1)}\frac{r}{\hat{r}}\right) \quad (1)$$

where $\hat{r} = \sqrt{E(R^2)}$ is the *rms* value of R, $E(\cdot)$ denotes statistical expectation, $I_v(\cdot)$ is the modified Bessel function of the first kind and order v, κ is the ratio of the dominant signal power to the scattered (multipath) power and μ is related to the number of multipath clusters.

The gamma distribution can be expressed in terms of a shaping parameter, α, and a scale parameter, β, as

$$p_Y(y) = \frac{y^{\alpha-1} e^{-\frac{y}{\beta}}}{\Gamma(\alpha)\beta^\alpha}, \quad y \geq 0 \quad (2)$$

where, is $\Gamma(\cdot)$ the gamma function. The κ-μ / gamma composite fading model can be expressed as the integral of the conditional distribution of the κ-μ fading with respect to the gamma shadowing as follows

$$p_X(x) = \int_0^\infty p_{R|Y}(r \mid Y = y) p_Y(y)\, dy \quad (3)$$

where, $p_{R|Y}(r \mid Y = y)$ is the κ-μ distribution with mode y and $p_Y(y)$ is the PDF of gamma distribution with parameters α and β. When (1) and (2) are substituted into (3)

and setting $r = x$ and $\hat{r} = y$, the κ-μ / gamma composite fading model can be written as follows

$$p_X(x) = \frac{2\mu(\kappa+1)^{\frac{\mu+1}{2}} x^\mu}{\kappa^{\frac{\mu-1}{2}} e^{\mu\kappa} \Gamma(\alpha) \beta^\alpha} \int_0^\infty \frac{I_{\mu-1}\left(2\mu\sqrt{\kappa(\kappa+1)}\frac{x}{y}\right)}{y^{\mu-\alpha+2} e^{\mu(1+\kappa)\frac{x^2}{y^2}} e^{\frac{y}{\beta}}} dy \quad (4)$$

Note that this equation corrects a typo in equation (7) of [12]. The term y^2 in (4) denotes mean squared power, which can be simply expressed as the sum of the dominant power and scattered power [9]

$$\hat{r}^2 = y^2 = E(R^2) = \delta^2 + 2\mu\sigma^2 \quad (5)$$

In this model, it is assumed that the mean squared value of fading amplitude is a gamma distributed random variable. Based on this assumption, (4) can be rewritten by letting u represent y^2 and performing a transformation of variables,

$$p_X(x) = \int_0^\infty p_{X|Y}(x|U=u)p_U(u)du$$

$$= \frac{2\mu(\kappa+1)^{\frac{\mu+1}{2}} x^\mu}{\kappa^{\frac{\mu-1}{2}} e^{\mu\kappa} \Gamma(\alpha) \beta^\alpha} \int_0^\infty \frac{I_{\mu-1}\left(2\mu\sqrt{\kappa(\kappa+1)}\frac{x}{\sqrt{u}}\right)}{u^{1-\alpha+\frac{\mu+1}{2}} e^{\mu(1+\kappa)\frac{x^2}{u}} e^{\frac{u}{\beta}}} du \quad (6)$$

IV. RESULTS

A. Path Loss

It is well known that the average received signal power decreases logarithmically with distance in both indoor and outdoor radio channels. The log-distance path loss for an arbitrary LOS transmitter-receiver separation is expressed as [13]

$$PL_{dB} = P(d_0) + 10\, n\, \log\left(\frac{d}{d_0}\right) \quad (7)$$

where, P is the path loss at the reference distance d_0, n is the path loss exponent which indicates the rate at which the path loss increases with distance, d is the distance between transmit and receive antennas. The path loss at the reference distance and path loss exponent were estimated using linear regression performed in MATLAB for both the LOS and NLOS walking scenarios. The reference distance for all scenarios was 1 m. Table I shows the parameter estimates for P and n for each transmitter location. It should be noted that all parameter estimates in Table I were obtained by taking the average values obtained for all three trials.

As expected, the path loss at the reference distance for NLOS was greater than that for LOS for all transmitter locations. Of the three transmitter locations, the wrist region recorded the least variation between path loss at the reference distance for LOS and NLOS. This observation may have been due to wrist region periodically alternating between LOS and NLOS channel conditions at the side and behind the body as the test subject was in motion. The lowest path loss at the reference distance was observed for the walking in LOS scenario when the transmitter was positioned on the waist. One possible reason for this could be that the height of both the waist mounted transmitter (1.15 m) and the receiver (1.10 m) were almost same, so the shortest path between transmitter and receiver was maintained while the test subject was walking.

TABLE I. ESTIMATED PATH LOSS AT THE REFERENCE DISTANCE AND PATH LOSS EXPONENT FOR EACH TRANSMITTER LOCATION FOR SCENARIOS 1 AND 2

	LOS		NLOS	
	$\overline{n}$	$\overline{P}$	$\overline{n}$	$\overline{P}$
Chest	1.04	47.9	0.17	60.1
Waist	1.82	43.1	0.34	65.6
Wrist	0.79	53.6	0.32	56.9

B. Shadowed Fading

To extract the shadowed fading, the estimated path loss, based on the test subject's velocity and the elapsed time, was removed from the measured data for scenarios 1 and 2, i.e. LOS and NLOS walking scenarios respectively. As the test subject only moved over very small distances in scenarios 3 and 4, the path loss was ignored and the global mean was removed from the raw data instead. All parameters for the κ-μ / gamma composite fading model were estimated using a non-linear least squares routine programmed in MATLAB. Table II shows the parameter estimates for the LOS and NLOS walking scenarios for each transmitter location. Please note that $\overline{\kappa}$, $\overline{\mu}$, $\overline{\alpha}$ and $\overline{\beta}$ are the mean parameter estimates averaged over the three repeated trials to improve their robustness. As expected, the values of α in LOS are greater than the ones in NLOS, meaning that the LOS walking case has less shadowing compared to the NLOS case. It can also be observed from the value of μ ($\mu < 1$) that these channels suffered less from multipath in this environment. Interestingly, the dominant signal component still existed even when the direct signal path was blocked by the test subject's body ($\kappa > 1$). This could have been caused by strong reflected signal components generated by metallic objects in the surrounding environment.

As an example of the results of the model fitting, Figs. 2 and 3 show the PDF of the κ-μ / gamma composite fading model fitted to the empirical data obtained for the waist positioned transmitter during the 2nd trial of the LOS and NLOS walking scenarios. The excellent fit of the composite fading PDF to the empirical channel data is clearly evident.

Furthermore, when visually compared to other popular fading models such as Rice and Nakagami-*m*, the *κ-μ* / gamma composite fading model provided the best fit for both LOS and NLOS walking scenarios.

		Parameters			
		$\overline{\kappa}$	$\overline{\mu}$	$\overline{\alpha}$	$\overline{\beta}$
Chest	LOS	1.54	0.84	7.54	1.83
	NLOS	4.18	0.64	2.25	1.93
Waist	LOS	6.82	0.54	4.50	1.55
	NLOS	5.53	0.52	1.78	2.14
Wrist	LOS	3.37	0.63	2.06	1.02
	NLOS	5.01	0.56	1.70	1.15

Fig. 2 Empirical PDF and *κ-μ* / gamma composite fading PDF for the waist positioned antenna in LOS walking scenario during the 2nd trial. For comparison, Rice and Nakagami-*m* PDFs are also presented.
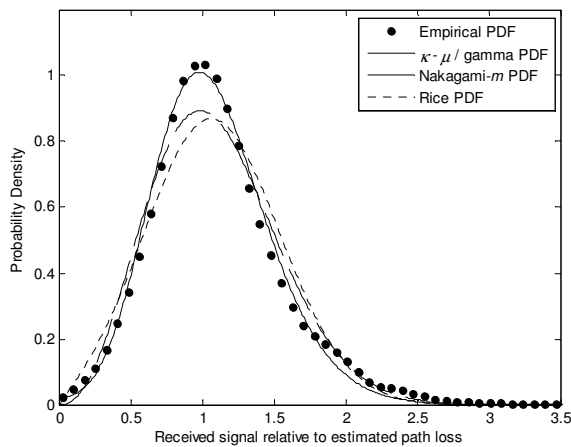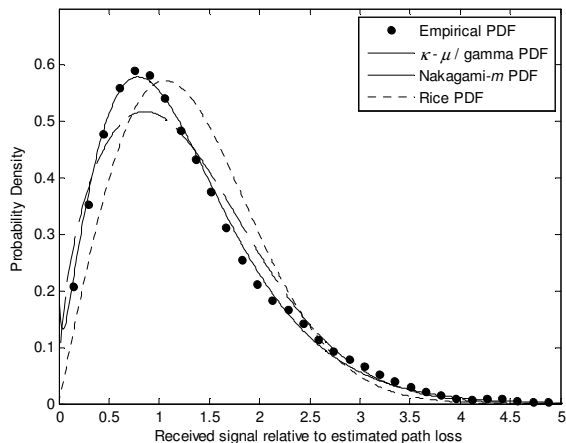

Fig. 3 Empirical PDF and *κ-μ* / gamma composite fading PDF for the waist positioned antenna in NLOS walking scenario during the 2nd trial. For comparison, Rice and Nakagami-*m* PDFs are also presented.

Table III shows the estimated parameters for the rotation and random movement scenarios when the transmitter was located on the central chest region. Again, the dominant signal component still existed for the rotation and random movement scenarios ($\kappa > 1$) except for the separation distance of 1 m. This trend also appears on the waist and wrist regions. This may be due to the short distance between the body worn node and receiver meaning that the received signal was more susceptible to shadowing due to the blocked LOS signal path while the test subject was rotating and moving randomly. This is evident from the estimated *α* parameter at 1 m which was smaller than that for 5 m and 9 m.

Interestingly, for the rotation scenario, as the distance between the body worn node and receiver increased, the estimated parameter *α* also increased, meaning that the received signal was less susceptible to shadowing. This may be explained considering that there are more multipath components which mitigate the body shadowing effect at separation distance of 5 m and 9 m compared to that at 1 m. For example, at the 9 m point the test subject was quite close to the corner of room. Thus we would expect a greater concentration of multipath due to signal components reflected by surrounding walls. The net result of this may have acted to mitigate the shadowing effect of the human body on the received signal.

As with scenarios 1 and 2, Figs. 4 and 5 show that the PDF of the *κ-μ* / gamma composite fading model provided an excellent fit to the empirical data for rotation and random movements (shown here at 5 m with the chest positioned transmitter). Again, when compared to other popular fading models such as Rice and Nakagami-*m*, the *κ-μ* / gamma composite fading model provided the best fit.

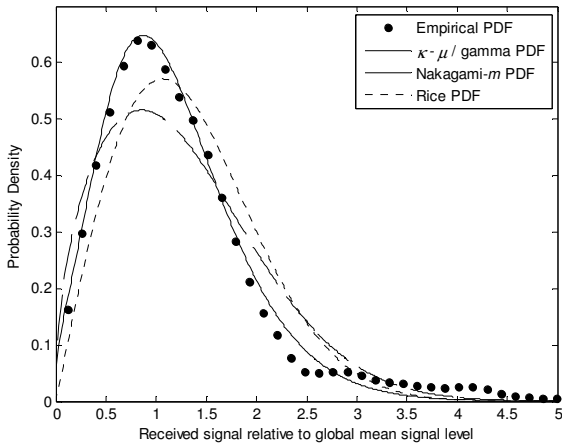|		Parameters			
		$\overline{\kappa}$	$\overline{\mu}$	$\overline{\alpha}$	$\overline{\beta}$
Rotation	1 m	0.01	0.99	1.08	3.17
	5 m	2.79	0.69	2.53	0.72
	9 m	5.71	0.66	6.03	0.49
Random	1 m	0.01	0.99	1.28	0.01
	5 m	1.46	0.85	2.05	1.46
	8 m	4.13	0.71	2.34	4.13

Fig. 4 Empirical PDF and κ-μ / gamma composite fading PDF for the chest positioned antenna in rotation movement scenario at 5 m during the 1ˢᵗ trial. For comparison, Rice and Nakagami-*m* PDFs are also presented.
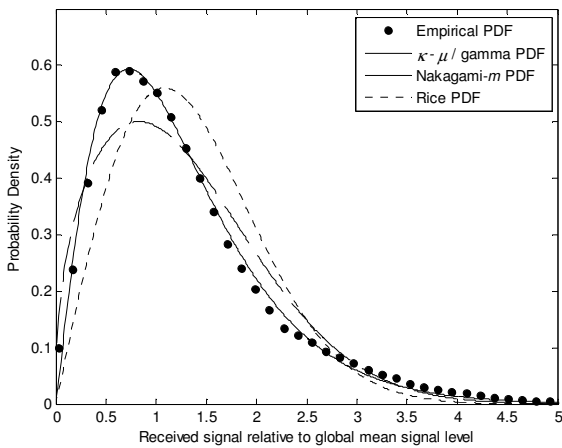

Fig. 5 Empirical PDF and κ-μ / gamma composite fading PDF for the chest positioned antenna in random movement scenario at 5 m during the 1ˢᵗ trial. For comparison, Rice and Nakagami-*m* PDFs are also presented.

V. CONCLUSIONS

The shadowed fading in off-body communications channels has been investigated using the κ-μ / gamma composite fading model. It's PDF has been shown to provide an accurate fit to the fading observed in measured off-body channels. It was found that a dominant signal component existed in all of the off-body channels investigated here. Furthermore they suffered less form multipath than shadowing. In a future contribution, we will further validate this model, for other types of body-centric communications such as on-body and body-to-body communications channels.

REFERENCES

[1] S. L. Cotton, A. McKernan, A. J. Ali and W. G. Scanlon, "An experimental study on the impact of human body shadowing in off-body communications channels at 2.45 GHz," *5th European Conference on Antennas and Propagation (EuCAP)*, pp. 3133-3137, Rome, Italy, Apr. 2011.

[2] Q. H. Abbasi, M. M. Khan, S. Liaqat, A. Alomainy and Y. Hao, "Ultra wideband off-body radio channel characterisation for different environments," *7th International Conference on Electrical and Computer Engineering (ICECE)*, pp. 165-168, Dhaka, Bangladesh, Dec. 2012.

[3] D. Smith, L. Hanlen, J. Zhang, D. Miniutti, D. Rodda and B. Gilbert, "Characterization of the dynamic narrowband on-body to off-body area channel," *IEEE International Conference on Communications (ICC)*, pp. 1-6, Dresden, Germany, June 2009.

[4] S. K. Yoo, S. L. Cotton and M. G. Doone, "Fading characteristics of indoor off–body communications with multiple–antennas at the base station," *IEEE APS URSI*, pp. 719-720 Memphis, USA, July 2014.

[5] C. Loo, "A statistical model for a land mobile satellite link," *IEEE Transaction on Vehicular Technology*, vol. 34, no. 3, pp. 122-127, August 1985.

[6] A. Abdi and M. Kaveh, "K distribution: an appropriate substitute for Rayleigh-lognormal distribution in fading-shadowing wireless channels," *Electronics Letters*, vol. 34, no. 9, pp. 851-852, April 1998.

[7] H. Suzuki, "A statistical model for urban radio propagation," *IEEE Transactions on Communications*, vol. 25, no. 7, pp. 673-680, July 1977.

[8] S. L. Cotton, "A statistical model for shadowed body-centric communications channels: theory and validation," *IEEE Transactions on Antennas and Propagation*, vol. 62, no.3, pp. 1416-1424, March 2014.

[9] M. D. Yacoub, "The κ-μ distribution and η-μ distribution", *IEEE Transaction on Antennas and Propagation*, vol. 49, no. 1, pp. 68-81, Feb. 2007.

[10] S. L. Cotton, "A statistical characterization of shadowed device-to-device communications in an indoor environment," *8th European Conference on Antennas and Propagation (EuCAP)*, The Hague, Netherlands, Apr. 2014.

[11] J. F. Paris, "Statistical characterization of κ-μ shadowed fading," *IEEE Transactions on Vehicular Technology*, vol. 63, no. 2, pp. 518-526, Feb. 2014.

[12] P. C. Sofotasios and S. Freear, "On the κ-μ / gamma composite distribution: A generalized multipath/shadowing fading model," *IEEE MTT-S International Microwave and Optoelectronics Conference*, pp. 390-394, Natal, Brazil, Nov. 2011.

[13] T. S. Rapport, Wireless Communications: principles and practices, New Jersey: Prentice Hall PTR, 2nd edition